



HAL
open science

Potential of the 15-Minute Peripheral City: Identifying Main Streets and Population within Walking Distance

Joan Perez, Giovanni Fusco

► **To cite this version:**

Joan Perez, Giovanni Fusco. Potential of the 15-Minute Peripheral City: Identifying Main Streets and Population within Walking Distance. Osvaldo Gervasi; Chiara Garau; David Taniar; Ana Maria A. C. Rocha; Maria Noelia Faginas Lago; Beniamino Murgante. Computational Science and Its Applications – ICCSA 2024 Workshops. Proceedings Part III., 14817, Springer, pp.50-60, 2024, Lecture Notes in Computer Science, 978-3-031-65237-0. 10.1007/978-3-031-65238-7_4 . hal-04863276

HAL Id: hal-04863276

<https://hal.science/hal-04863276v1>

Submitted on 3 Jan 2025

HAL is a multi-disciplinary open access archive for the deposit and dissemination of scientific research documents, whether they are published or not. The documents may come from teaching and research institutions in France or abroad, or from public or private research centers.

L'archive ouverte pluridisciplinaire **HAL**, est destinée au dépôt et à la diffusion de documents scientifiques de niveau recherche, publiés ou non, émanant des établissements d'enseignement et de recherche français ou étrangers, des laboratoires publics ou privés.

Potential of the 15-Minute Peripheral City: Identifying Main Streets and Population within Walking Distance

Joan Perez ^[0000-0003-3003-0895] and Giovanni Fusco ^[0000-0002-6171-5486]

Princeton University, Princeton NJ 08544, USA
Université Côte-Azur – CNRS – AMU – AU, ESPACE, France.
joan.perez@univ-cotedazur.fr

Abstract. The concept of the 15-minute city presents challenges for pedestrian accessibility, particularly in peripheral areas with less pedestrian-friendly street networks. This paper explores the angular continuity of main streets and the population potential around them as crucial elements for the development of the 15-minute peripheral city. By utilizing geoprocessing algorithms, the study aims to identify main streets and verify their demographic potential in two distinct geographic contexts near Lille and Nice, France. The protocol is divided into four steps, as follows: (1) main streets identification through continuity, (2) calculation of morphological indicators on buildings, (3) machine learning to estimate the number of dwellings per building, and (4) population potential estimate within different walking distances from main streets. The findings reveal a network of interconnected main streets with significant population potentials in the outskirts of both test areas. These streets could serve as the development corridors for enhancing commercial activities and services, supporting the vision of the 15-minute city in peripheral areas.

Keywords: 15-minute city, street network, catchment area, pedestrian accessibility, angular continuity.

1 Introduction

The 15-minute city poses a challenge to pedestrian accessibility, particularly in the outskirts and peripheries where the street network is less pedestrian-friendly. The Evolutionary Meshed Compact City (emc2¹) project proposes a new model of the 15-minute city for the loose structural networks of peripheral location (Fusco *et al.*, 2023). It envisages compact urban forms as corridor developments based on existing main roads, forming a meshed structure within metropolitan areas. The emc2 project is currently working on the characterization of morphological and demographic preconditions for these developments. The present paper is a first proposal in this direction, focusing on two specific aspects: angular continuity of main streets and population potential in a wider area around them. Indeed, in addition to numerous challenges for the 15-minute city to work effectively, such as inclusive urban design exemplified by the creation of walkable neighborhoods, conditions have to be met for the presence of retail and

¹ <https://emc2-dut.org/>

services. Building on the theory of natural movement (Hillier *et al.*, 1993), the emc2 model considers a first requirement the existence of a well-connected foreground network of main streets, where retail and services can cluster. However, this begs the question of the potential demand within a walking catchment area, to ensure the presence of proximity-based activities. It becomes thus important to both identify possible elements of the foreground network of main streets and verify that they benefit from the demographic potential to become the backbone of the 15-minute peripheral city. Specific geoprocessing algorithms are needed to achieve these goals, as those presented and discussed within this paper.

For this paper, we decided to focus on two distinct geographic contexts situated on the outskirts of the metropolitan areas of Lille and Nice, in northern and southern France, respectively. The considered outskirts of Lille is made of the following 4 municipalities: Santes, Hallennes-lez-Haubourdin, Haubourdin, and Emmerin, totally accounting for 27.993 inhabitants over² 22.2 km²; while within the outskirts of Nice we focused on the municipalities of Drap, Cantaron and La Trinité accounting for 16.572 inhabitants over 27.8 km². Building footprints, roads, and administrative boundaries are extracted from the version 3.3 of the French dataset BD TOPO®³ (IGN, 2023). These two case studies provide interesting geographical differences: a flat terrain with a tradition of linear developments around Lille as opposed to a more constrained hilly landscape where topography induces linear developments around Nice.

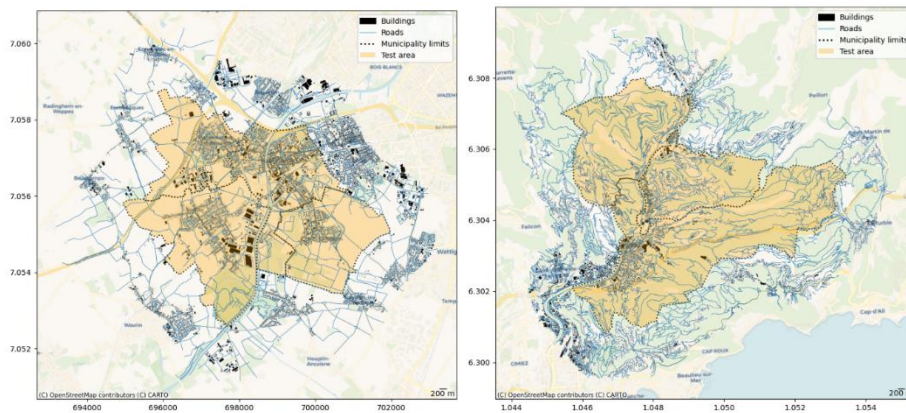


Fig. 1. Test areas, the municipalities of Santes, Hallennes-lez-Haubourdin, Haubourdin, and Emmerin in the the outskirts of Lille (left) and Drap, Cantaron and La Trinité in the outskirts of Nice (right)

² INSEE, 2020 : Territory comparator <https://www.insee.fr/fr/statistiques/1405599?geo=COM-59286+COM-59278+COM-59193+COM-06054+COM-06031+COM-06149>

³ Version 3.3 of the BD TOPO® <https://geoservices.ign.fr/bdtopo#telechargementpgkgreg>

A buffer of 1200 meters (see catchment areas **Section 5**) has been performed over the administrative boundaries of the test areas in order to include 37.985 buildings and 6.157 road segments in the Lille outskirts, and 24.001 buildings and 6.179 road segments in the Nice outskirts. Highways and highway ramps are manually filtered out of the dataset, as they cannot play the role of pedestrian-friendly main streets for the 15-minute city. In addition, dual carriageways are re-digitized as single carriageways to improve the performances of the identification of main streets (**Section 2**). This paper is organized as follows. **Section 2** presents the identification of main streets through an improvement of the *Morpheo*'s algorithm. **Section 3** focuses on the computation of morphometric indicators over buildings. **Section 4** uses machine learning (classification + regression) to estimate the number of dwellings per building. **Section 5** estimates the population potential around the identified main streets through catchment areas consistent with the 5, 10 and 15 minute-city. **Section 6** concludes the paper with a discussion regarding future improvements of the protocol. Input data and the protocol are fully reproducible and available (see **Section 6**).

2 Main streets through continuity

Angular continuity is useful for defining main streets and is normally assessed through intersection continuity negotiation algorithms (Porta *et al.*, 2006). The QGIS plugin *Morpheo* (Lagesse, 2015) proposes a specific algorithm to assemble angularly continuous street segments in new objects called “ways” (i.e. natural streets, Stavroulaki *et al.*, 2017) and hierarchizes them through connectivity measures. Aggregation of street segments uses deletion buffers at segment intersections and deviation angles. After applying the *Morpheo* plugin with the preconized parameters (deletion buffer of 4 meters, deviation angles of 60°) over the two test areas, we obtain 1.891 ways for the outskirts of Lille, and 2.006 for the outskirts of Nice. Our proposal extends *Morpheo*'s algorithm, acknowledging that peripheral areas have normally ways with lower values of connectivity than those in central areas. To identify main streets in a local context, we introduce a novel indicator considering the connectivity of surrounding ways: the local relative connectivity ($CONN_{LocRel}$). Its purpose is to identify segments with connectivity levels significantly different from their immediate surroundings, highlighting potential connectivity anomalies which become focal elements in local contexts. Prior to calculating the local relative connectivity, two indicators have to be calculated.

$$CONN_{LocSum} = \sum_{i=1}^n CONN_i$$

$$CONN_{LocAvg} = \frac{CONN_{LocSum}}{n}$$

$$\text{CONN}_{\text{LocRel}} = \frac{\text{CONN}}{\text{CONN}_{\text{LocAvg}}}$$

where CONN_i represents the sum of connexity values associated with each intersecting buffer, n the number of intersecting segments and CONN the connexity value of a given segment.

The first indicator is the sum of the connexity values associated with all intersecting buffers for each way identified by *Morpheo*. This indicator, named $\text{CONN}_{\text{LocSum}}$, reflects the overall level of connectivity for individual road segments. Moving on, the second indicator, $\text{CONN}_{\text{LocAvg}}$, considers the number of intersecting segments when calculating connexity, thereby providing a weighted average connexity value for each of them. Finally, the local relative connectivity ($\text{CONN}_{\text{LocRel}}$) computes *Morpheo* connexity standardized by $\text{CONN}_{\text{LocAvg}}$. This indicator evaluates connexity relative to the local connectivity context, allowing for the identification of segments with disproportionately high connexity values compared to neighboring segments.

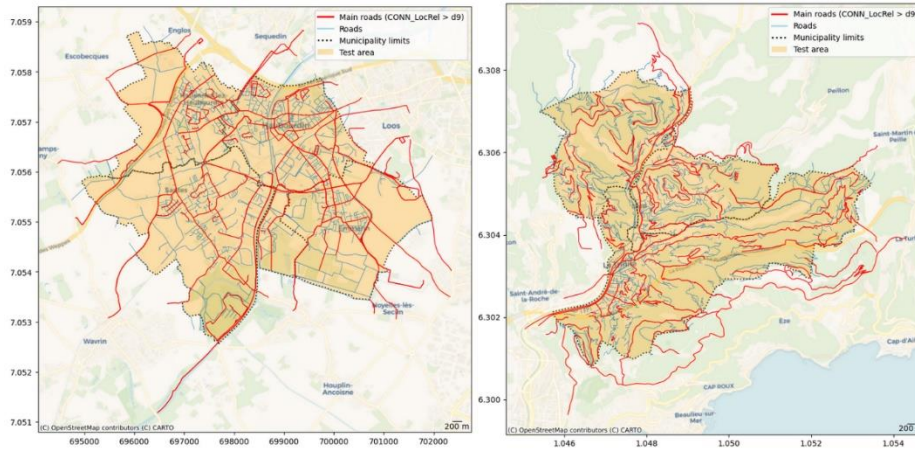


Fig. 2. The main roads in the outskirts of Lille (left) and Nice (right)

Figure 2 illustrates the identification of the main streets in the test areas within the test regions by mapping the segments characterized by a $\text{CONN}_{\text{LocRel}}$ value falling within the 10th decile. In both the outskirts of Lille and Nice, results appear consistent with a successful identification of segments with high connexity values compared to neighboring segments. These street segments will serve as the focal elements for aggregating population potentials, as outlined in **Section 5**. In Lille, the D9 value is 1.26, whereas in Nice, it is 1.33. Populations will be estimated from dwelling data. However, the number of dwellings is not available for some buildings (see further), which forces us to first implement some morphological indicators (**Section 3**) to assign them an estimated number of dwellings.

3 Morphological indicators

This section is about the calculation of diverse indicators associated with building morphology. The goal is to collect enough morphological indicators to subsequently assess whether a building contains dwellings or not (**Section 4**). The premise is that buildings with dwellings, whether entirely residential or mixed-use, exhibit distinct morphological characteristics compared to non-residential structures (Steadman 2014, Araldi *et al.*, 2023, Perez *et al.*, 2024). For instance, industrial and logistic buildings often have larger footprints, while their shapes may demonstrate reduced elongation and high convexity, reflecting specific requirements related to their function. Basic indicators, such as surface areas or perimeters are computed using *geopandas*. For advanced indicators, like the ratio of shared walls or the elongation of each building, we use the urban morphology toolkit *momepy*, a library for quantitative analysis of urban form developed by Fleischmann (2019).

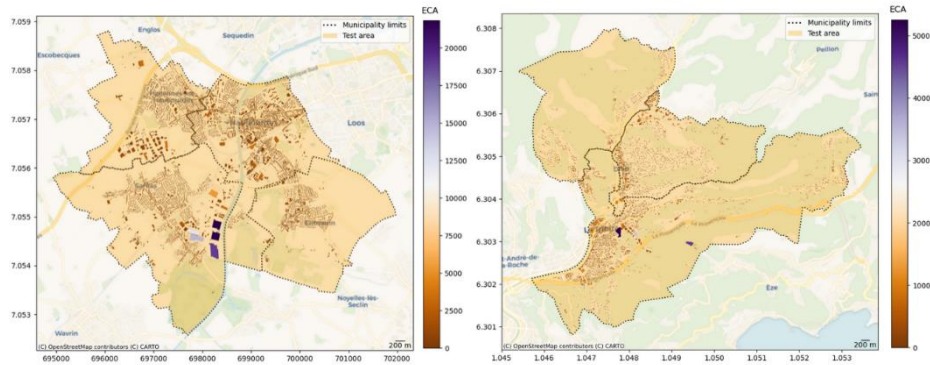


Fig. 3. ECA (Elongation-Convexity-Area) values per building in both test areas

We also derive three composite indicators, based on the basic metrics previously calculated. The first, denoted FA (Floor-Area) is the product of floor and area ($F \cdot A$). ECA (Elongation-Convexity-Area), is made to discern sizable yet non-elongated specialized structures/instances often characteristic of non-residential buildings, distinct from elongated modernist residential complexes.

$$ECA = (1 - E) \cdot C \cdot A$$

As displayed in **Figure 3**, large sized but yet non-elongated buildings are well detected by the ECA indicator. Then, EA (Elongation-Area), which is the product of surface area and elongation ($E \cdot A$), shall assume significance in estimating the number of dwellings per building. The final feature attributes of the dataset are as follows: F (number of floors), A (surface area of the building footprint), P (perimeter), E (elongation), C (convexity), FA (floor-area), ECA (elongation-convexity-area), EA (elongation-area) and SW (shared walls).

4 Dwellings estimation

The goal of this section is to estimate the number of dwellings per building based on the morphometry indicators that have been calculated in the previous section. We proceed with two main tasks: classification for evaluating the presence of dwellings and regression for estimating the number of dwellings.

For classification, we use a decision tree classifier to predict whether a building has dwellings or not, based on its morphology indicators. The attribute data from the BD TOPO@ contains the number of dwellings per building. Yet, this feature is incomplete. For example, in the Lille subset, 45.93% of the information is missing, while in Nice it reaches 60.11%. We isolate these buildings. Subsequently, for the remaining buildings, a binary encoding is applied: buildings without dwellings are assigned a value of 0, while buildings with dwellings are assigned a value of 1, irrespective of the actual count of dwellings within each building. The datasets for Lille and Nice are partitioned into training (70%) and testing (30%) subsets.

Table 1. Decision tree classifier performance metrics for Lille and Nice subsets

	Complexity Param	N_Splits	Predicted	Expected	Accuracy
Lille subset					
	0.658247	0	1	0.1818	0.9549
	0.013585	1	0	0.0572	
	0.013139	3	1	0.0629	
	0.011736	6	1	0.0436	
	0.010000	9			
Nice subset					
	0.322142	0	1	0.2089	0.8795
	0.028928	1	0	0.0922	
	0.017142	3	1	0.0922	
	0.012142	6	1	0.0922	
	0.011666	7			
	0.010000	10			

The trained model's accuracy is then evaluated against the test subset using confusion matrices. The proportion of correctly classified instances reaches 95.49% for the subset in Lille, and 87.95% for the subset in Nice, which indicated a relatively good overall performance of the decision tree classifier. Other performance metrics are provided in **table 1**, such as the complexity parameter, the number of splits, predicted and expected values. As the number of splits increases, the model becomes more specific in its predictions.

Table 2. Decision tree classifier: variable importance for Lille and Nice subsets

Feature	Lille subset	Nice subset
FA	36	34
A	28	26
P	27	23
ECA	4	7
EA	4	8
SW	1	0
E	1	0

As evidenced in **Table 2**, Floor-Area, Area and Perimeter emerge as the most influential variables in determining the presence of dwellings within buildings, with ECA and EA contributing less often, i.e. for more specific subsets of buildings. The models' performance is considered sufficiently robust to extend their application to buildings with missing information regarding dwelling presence, which were identified earlier in this section. The next step is to estimate the number of dwellings for buildings that lack information but have been identified as possessing dwellings by the decision tree classifier. Those buildings are temporarily isolated. Subsequently, we set up a repeated k-fold cross-validation framework to train a stepwise regression model using the *leap-Backward* method from the caret library (Kuhn *et al.*, 2023). The morphology indicators are used as predictors, while the target variable is the number of dwellings.

Table 3. Stepwise regression performance metrics

nvmax	Nice subset			Lille subset		
	RMSE	R ²	MAE	RMSE	R ²	MAE
1	4.422	0.724	1.324	2.056	0.771	0.654
2	4.100	0.755	1.814	2.062	0.771	0.639
3	4.135	0.751	1.805	2.085	0.765	0.646
4	4.058	0.759	1.732	2.051	0.775	0.631
5	4.065	0.759	1.719	2.040	0.777	0.666
6	4.066	0.759	1.718	2.050	0.775	0.688
7	4.052	0.760	1.705	2.027	0.779	0.705

As the maximum number of variables allowed and incorporated into the regression model increases (nvmax), there is a trend of decreasing Root Mean Squared Error (RMSE) and increasing coefficient of determination (R²), indicating a better fit of the model. **Table 3** illustrates this trend, also showing slightly higher RMSE values in the Nice subset compared to the Lille subset, accompanied by lower R² values, suggesting slightly better accuracy in Lille. However, with R² values above 0.7 in both models, the overall performance indicates that the model is effective in estimating the number of dwellings per building. In Nice, the coefficient of determination does not show

improvement beyond four regressors. Conversely, in Lille, the gain is negligible, with an increase of only 0.002. Therefore, we will opt for a model with four regressors.

Table 4. Stepwise regression variable importance

nvmax	F	A	P	E	C	FA	ECA	EA	SW
Lille subset									
1						*			
2	*					*			
3	*	*				*			
4	*	*				*	*		
5	*	*		*		*	*		
6	*	*	*	*		*	*		
7	*	*	*	*	*	*	*		
Nice subset									
1						*			
2						*		*	
3						*	*	*	
4		*				*	*	*	
5	*	*				*	*	*	
6	*	*	*			*	*	*	
7	*	*	*	*		*	*	*	

Table 4 shows that for four regressors, the number of floors (F), area (A) and floor-area (FA) are significant in both models. For the fourth regressor, elongation-convexity-area (ECA) is better for Lille and elongation-area (EA) for Nice. Since elongation-area (EA) is never significant for Lille, a linear formula is created on floors (F), area (A), floor-area (FA) and elongation-convexity-area (ECA). We then generate the predictions for the number of dwellings and ensures that negative predictions (resulting from sparse data) are adjusted to 0. Finally, the estimated dwelling numbers are assigned to buildings lacking information about dwellings but identified as possessing dwellings by the decision tree classifier.

5 Catchment areas and population potentials

This section focuses on estimating the population potential within catchment areas around main axes. It begins by importing the main roads as identified as the 10th decile from the Connexity indicator in **Section 2** and the buildings with the estimated number of dwellings from **Section 4**. Catchment areas are created around the main roads using buffers of 400, 800 and 1200 meters. 400, 800 and 1200 meters roughly corresponds to 5, 10 and 15 minutes of walking time for able-bodied adults. Population potential per building is then calculated based on the estimated number of dwellings, considering an average household size of 1.92 for collective housings and 2.44 for single-family homes in France (Léger, 2019). The methodology aggregates the population count of each building to the catchment areas within the three specified catchment radii. Values are

subsequently spatially joined to the main roads thus providing population potentials along the latter as highlighted below.

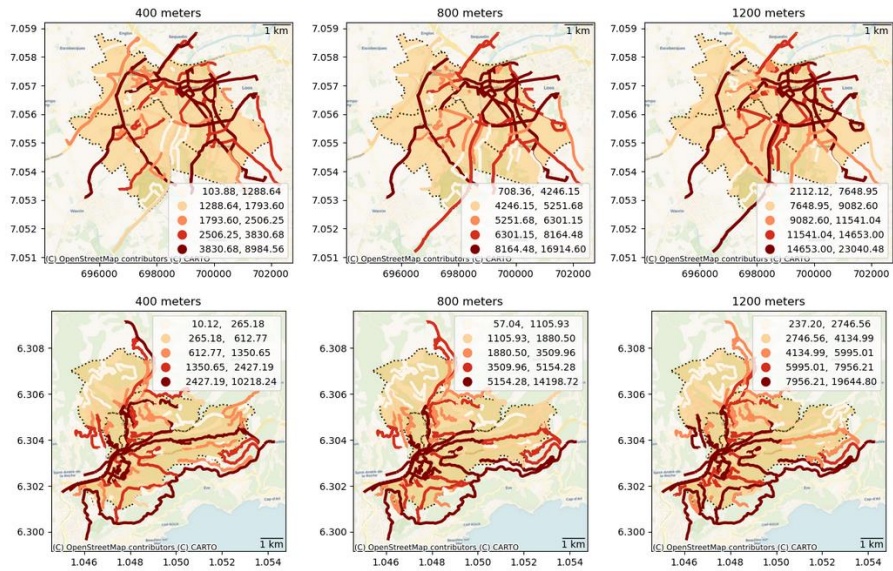


Fig. 4. Population potentials along main axes in the outskirts of Lille (top) and Nice (bottom) for catchment radii of 400, 800 and 1200 meters

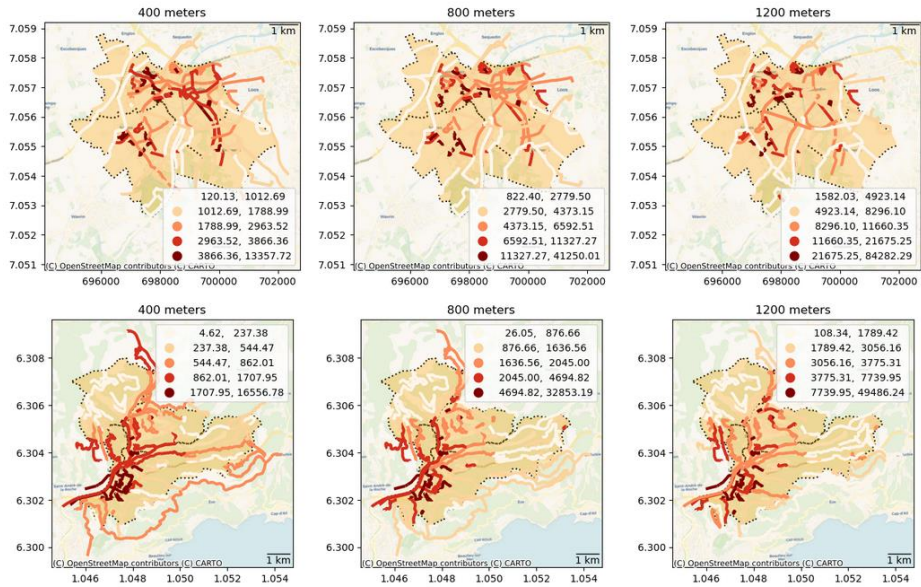


Fig. 5. Population potentials per kilometer of road along main axes in the outskirts of Lille (top) and Nice (bottom) for catchment radii of 400, 800 and 1200 meters

Figure 4 also shows that a meshed structure of main streets clearly appears in the outskirts of Lille. Main streets also stand out in the outskirts of Nice but due to the topology and to numerous valley dead ends, a meshed structure is less evident. The relative population potentials, standardized per kilometer of road (**Figure 5**), highlight focal points and smaller meshed segments with advanced demographic preconditions for the development of the emc2 model.

6 Catchment areas and population potentials

The findings are in line with the real-world situations in both the outskirts of Lille and Nice and with our intended objective: identifying a network of interconnected main streets with population potentials conducive to targeted densification efforts. These identified main streets could serve as the backbone for enhancing commercial activities, services, and amenities in the area. Yet, we stress on the importance of investigating other factors, such as population heterogeneity or kinds of services/retail activities. The protocol has been made available on GitHub (**Appendix 1**) and the datasets for Lille and Nice on Zenodo (**Appendix 2**). On Zenodo, both inputs and outputs are available within two GeoPackages. The protocol is divided into 4 main steps and one appendix as follows: (1) the identification of main streets - R Script (2) morphometry on buildings - Python script (3) evaluation of the number of dwellings within inhabited buildings - R Script (3) projecting population potential to main streets - R Script (Appendix) thematic maps presented in this paper - Python script.

The protocol outlined in this paper represents an exploratory phase, providing preliminary results derived from two extremely different geographical contexts. It is clearly subject to several improvements that we would like to discuss in what follows. Firstly, angular continuity analysis shall be combined, or replaced by configurational analysis that is used to identify what is described as the foreground network (i.e. main streets) in space syntax research; Hillier, 1996). More specifically, the multiscale configurational protocol proposed by Berghauser Pont *et al.*, (2019) allows for the identification of local main streets with no regards to the street typology. Since we manually filtered highway and highway ramps (**Section 1**), configurational analysis could significantly improve the protocol. Second, the morphology indicators could be calculated at different spatial lags in order to add indicators for the classification and regression models. Spatial lags could help detecting buildings that are exceptions amongst local areas. Third, the null hypothesis of complete spatial randomness (CSR) shall be tested regarding the distribution of buildings with missing values of dwellings. Fourth, the estimation of the number of dwellings per building could be improved with, for example, using a count regression model for which the value zero cannot occur, such as the zero-truncated Poisson or negative binomial regressions. The population assigned to the different dwelling types could also be calculated with more place specific data and should be validated with available disaggregated census data to consider the presence of dwelling units used as secondary homes. Lastly, while catchment areas are currently calculated using Euclidean distance, employing network distance would yield more precise outcomes, given that individuals walk along paths and streets.

Acknowledgments. This paper is part of the emc2 project, which received the grant ANR-23-DUTP-0003-01 from the French National Research Agency (ANR) within the DUT Partnership.

References

1. Araldi, A., Emsellem, D., Fusco, G., Tettamanzi A. and Overall D. (2023) Building types in France. Clustering building morphometrics using national spatial data, *Revue Internationale de Géomatique*, ISSN 1260-5875, 31, 3-4 (2022), pp. 265 – 302, <https://doi.org/10.3166/rig31.265-302>
2. Berghauser Pont, M., Stavroulaki, G., Bobkova, E., Gil, J., Marcus, L., Olsson, J., Sun, K., Serra, M., Hausleitner, B., Dhanani, A., & Legeby, A. (2019). The spatial distribution and frequency of street, plot and building types across five European cities. *Environment and Planning B: Urban Analytics and City Science*, 46(7), pp. 1226-1242.
3. Fleischmann, M. (2019) ‘momepy: Urban Morphology Measuring Toolkit’, *Journal of Open Source Software*, 4(43), p. 1807. doi: 10.21105/joss.01807.
4. Fusco, G., Berghauser Pont M., Cutini V., Psenner A., 2023, The Evolutive Meshed Compact City – A new framework for the 15mC in peripheral areas, *Proceedings of ECTQG2023*, Braga, pp. 85-87. https://ucpages.uc.pt/site/assets/files/1249198/ectqg_2023_proceedings_final.pdf
5. Hillier B., Penn A., Hanson J., Grajewski T. Xu J. (1993) Natural movement: or, configuration and attraction in urban pedestrian movement. *Environment and Planning B: Planning and Design*, 20, 29-66.
6. Hillier B. (1996) *Space is the machine*. Cambridge University Press, Cambridge.
7. IGN (2023) *BD TOPO® Version 3.3*, Descriptif de contenu. Institut national de l'information géographique et forestière, 387 p.
8. Kuhn, M. (2023). Package ‘caret’: Classification and Regression Training (Version 6.0-94) [Software]. <https://github.com/topepo/caret/>
9. Lagesse, C. (2015) *Lire les Lignes de la Ville : Méthodologie de caractérisation des graphes spatiaux*. Géographie. Université Paris Diderot-Paris VII, Thèse, 566 p.
10. Léger, J.-F. (2019). Le lien logement-population à l'échelle locale. I – Le « rendement démographique » des logements. *Espace populations sociétés*, 2019/3.
11. Perez, J., Fusco, G. and Sadahiro, Y. (2024) Population and Morphological Change: A Study of Building Type Replacements in the Osaka-Kobe City-Region in Japan. *Geographical Analysis, Early View*, Online Version of Record before inclusion in an issue.
12. Porta, S., Crucitti, P. and Latora, V. (2006) The network analysis of urban streets: A dual approach. *Physica A: Statistical Mechanics and its Applications*, 369(2), pp. 853-866.
13. Stavroulaki, I., Marcus, L., Berghauser Pont, M. and Carl Staffan Nilsson, L. (2017) Representations of street networks in space syntax towards flexible maps and multiple graphs, 11th International Space Syntax Symposium, SSS 2017, Lisbon, Portugal, 3-7 July 2017, 5: 174.1-174.16.
14. Steadman, P. (2014). *Building types and built forms*. Troubador Publishing Ltd.

Appendix 1

Metadata and links for codes on GitHub to be added – ½ page

Appendix 2

Metadata and links for datasets on Zenodo to be added – ½ page